GLASS FIBER-REINFORCED PLASTIC POLES FOR TRANSMISSION AND DISTRIBUTION LINES: AN EXPERIMENTAL INVESTIGATION

D. Polyzois , S. Ibrahim, V. Burachynsky, and S. K. Hassan

Department of Civil and Geological Engineering, University of Manitoba, Winnipeg, MB, R3T 2N2,Canada

SUMMARY: An extensive research project is currently being carried out at the University of Manitoba, Canada, to develop lightweight glass fiber-reinforced plastic (GFRP) poles for use in transmission and distribution lines. In this paper, results from tests involving full-scale tapered GFRP poles with hollow a circular cross-section subjected to cantilever bending are presented. The filament winding process was employed to produce those poles using vinylester resin reinforced with E-glass fibers. Twelve bending tests were conducted on full-scale poles up to failure. Test parameters included fiber orientation and number of layers. Extensive theoretical work preceded the test program and a theoretical model was developed. The results to-date indicate that the developed theoretical model can predict quite well the ultimate capacity and behavior performance of GFRP poles.

KEYWORDS: Transmission and distribution poles, filament winding, fiber-reinforced plastics.

INTRODUCTION

Traditional materials such as wood, steel, and concrete are commonly used to construct electrical transmission and distribution poles. However, the shortage of wooden poles, their short life expectancy, and various environmental concerns have promoted hydro-electric utility companies to search for a cost-effective alternative. Wooden poles are continuously exposed to weather, fungi, woodpeckers, etc., which result in a very significant deterioration of their load bearing capacity with the time. The service life of wooden poles is approximately 20 years [1]. Any extension of this service life requires continuous inspection and follow-up care. In a number of European countries, concrete poles are used. The main disadvantage of concrete poles is their weight, which drastically increases transportation and erection costs. Chemical influences on the concrete surfaces due to environmental impact can also affect their long term performance. As in the case of other concrete structures, concrete poles are subject to corrosion of the steel reinforcement, resulting in further strength deterioration and expensive maintenance. Steel is the most common material for the construction of transmission poles in North America. These poles, however, are very expensive. Corrosion protection is of primary concern in steel poles which must be painted or galvanized, a process which does not always

guarantee long term protection. Generally, traditional poles made of wood, concrete, or steel are subject to deterioration under environmental attacks. Regular maintenance is essential to prolonging serviceability of these poles.

On the other hand, Glass Fiber-Reinforced Plastic (GFRP) poles are lightweight and corrosion resistant. Being lightweight is a major advantage of GFRP poles making them suitable for transportation and installation in mountain terrains and marshes. Although the initial cost of GFRP poles may be higher than traditional poles, the long term benefits these poles provide, make their selection attractive. The use of GFRP poles is not new. A number of companies are already involved in the production of such poles. Research in this area, however, is limited.

In 1988, Bell initiated its own investigation of GFRP poles, and conducted an experimental program at the Centre de Recherche du Reseau Exterior (CERRE) [2]. The specimens were tapered with hollow cross section and were manufactured by centrifugal casting. The test results indicated that GFRP poles could safely resist loads comparable to those of wooden poles. The behavior of these GFRP poles was found to be truly elastic even for large deflections.

An experimental investigation was also conducted by Shakespeare Inc. on filament wound GFRP poles in 1993 [3]. Class 4 GFRP poles were tested at the national test labs of Engineering Data Management (EDM) in Colorado, USA. The tests were successful as each pole met or exceeded the strength requirement specified for wooden poles.

The research program at the University of Manitoba, Canada, was to:

a) develop a theoretical model for determining the ultimate strength and performance of GFRP poles;

b) evaluate the developed theoretical model through a series of small and full-scale testing; and

c) develop design guidelines for the use of GFRP.

To-date, twelve small scale specimens (2.5 m long) and twelve full-scale specimens (6.25 m long) have been tested under cantilever bending load up to failure. This paper presents the results from the full-scale tests.

EXPERIMENTAL PROGRAM

Specimens and Test Setup

The poles were fabricated through the filament winding wet process at the ISIS-Faroex Filament Winding Research Facility. E-glass fibers and vinylester resin (DERAKANE 470-300) were used for manufacturing these poles. The material properties and strength for both the fiber and the resin were provided by the manufacturer [4] and are presented in Table (1).

Table 1: Properties of E-Glass and Vinylester resin

Properties	E-Glass	Vinylester resin (DERAKANE 470-300)
Tensile modulus (GPa)	72.4	3.58
Poisson's ratio	0.2	0.3
Tensile Strength (MPa)	2400	85
Shear Modulus (GPa)	30	1.38
Density (gm/cm^3)	2.54	1.08

The specimens were tapered hollow sections, 6250 mm in length. The inner diameters at the base and at the top were 416 mm and 305 mm, respectively. The wall thickness for each specimen varied depending on the number of layers, which ranged from 4 to 8, in two layer increments, giving a total thickness of between 2.75 mm and 5.5 mm at the base. Three fiber angles with respect to the longitudinal axis of the pole were used: 5/-5, 10/-10, and 20/-20. Hoop winding was also employed in ten of the specimens with different ratios, while only two of the specimens were fabricated without hoop winding. The fiber volume fraction was measured during the manufacturing process by determining the weight of fiber and resin used and transforming those weights into volume fractions. The configurations as well as the fiber volume fraction for the tested specimens are listed in Table (2).

Table 2: Configuration and fiber volume fraction of full-scale specimens

Specimen Number	Longitudinal Fiber Orientation	Number of Hoop Layers	Total Number of Layers	Base Thickness (mm)	Fiber Volume (%)	Total Weight (Kg)
1	(10/-10)	0	8	5.5	49	99.40
2	(10/-10)	2	8	5.0	60	80.25
3	(10/-10)	4	8	4.5	60	68.15
4	(10/-10)	2	6	4.0	54	60.85
5	(10/-10)	2	4	2.4	60	39.00
6	(20/-20)	0	8	5.5	53	94.30
7	(20/-20)	2	8	5.0	60	81.00
8	(20/-20)	4	8	4.9	58	72.05
9	(20/-20)	2	6	4.0	57	59.40
10	(20/-20)	2	4	2.75	51	38.20
11	(5/-5)	2	6	4.6	50	62.50
12	(5/-5)	2	4	2.8	52	38.00

The fixed support for the specimens consisted of a square reinforced concrete base measuring 800 mm wide by 1000 mm high. It was made up of two segments with a tapered circular hole in the middle with dimensions that matched the outer diameter of the specimens. The two segments of the base were clamped together using four dwyidag bars, as shown in Fig. 1. To insure the stability of the portion of the specimen within the base, a GFRP tapered sleeve, 1000 mm long, and 25 mm thick, was inserted in the specimen. The concrete base was clamped to a rigid structural wall using four hollow square steel (HSS) sections (250 x 250x 6 mm), two on each side of the base, as shown schematically in Fig.1. Four high strength

dwyidag bars were used to clamp the HSS section and the concrete base to the structural wall. To ensure full fixity of the specimen within the concrete base, the gap between each specimen and the concrete base was filled with plaster of Paris.

The load was applied horizontally, 600 mm below the top, according to the ANSI standard [5]. An electronic load cell was used to monitor the applied load, as shown in Fig. 1. Loading was applied at a rate of approximately, 0.25 mm/second.

The lateral deflection of the poles at the loading position was monitored through an electronic linear measurement transducer (LMT). The LMT was mounted on a fixed steel column 10000 mm away from the specimen. The stroke range for each LMT is 2500 mm.

Two LMTs attached on two opposite sides of the poles, approximately, 1000 mm above the base, were used to monitor the change in the specimen diameter, as shown in Fig.1. These LMTs had a range of 350 mm. The difference between the readings between the two LMTs represented the change of the specimen diameter at that height. This method allowed continuous monitoring of the change in the diameter with loading.

Strain along the specimen near the base was monitored through 24 electrical resistance strain gauges. The strain gauges had 5 mm gauge length and 120 ohm electrical resistance. Three strain gauges were mounted at eight different locations, to measure strains in the longitudinal, circumferencial and 45 degrees off-axis. Four strain gauges were located on tension side and the other four on the compression side at heights 30, 400, 800, and 1200 mm above the concrete base.

The load cell, the LMTs, and the strain gauges were connected to a computer controlled 32 channel Data Acquisition System to monitor and record all data. Visual observations were also made during the test. The load was applied until complete failure of the specimen occurred.

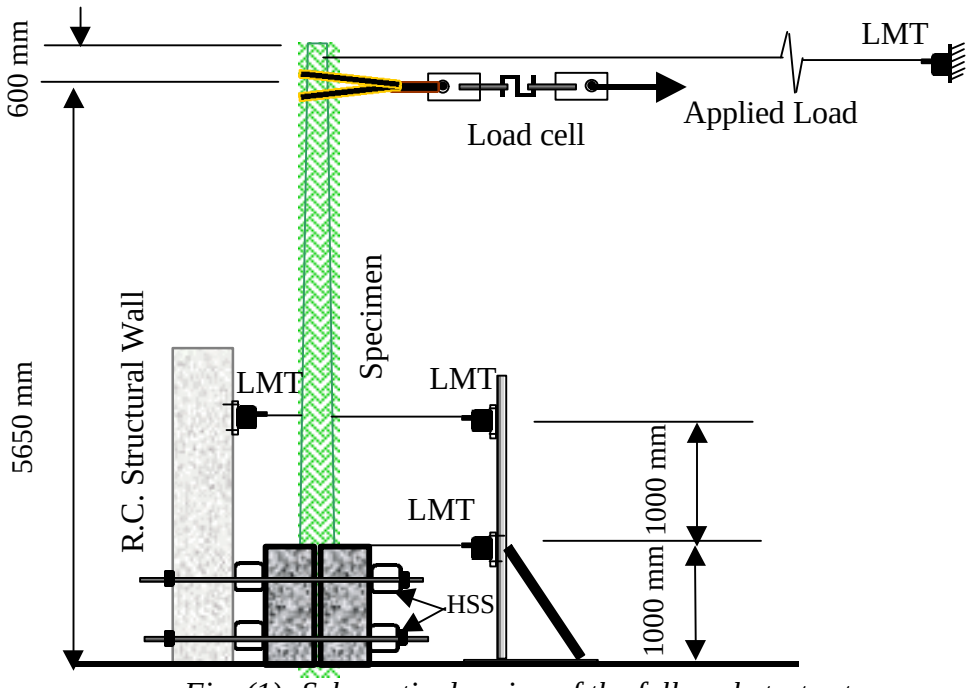

Fig. (1): Schematic drawing of the full-scale test setup

Test Results

A summary of all test results is shown in Table (3). The equivalent wooden pole class is also shown in this table. It should be noted that specimen 2 failed prematurely inside the concrete base because no internal stiffener was used for that specimen. Two specimens (4, and 11) satisfied the requirement of class 1 pole, according to Ref.(5), by carrying an ultimate load equal to or exceeding 20 KN (4500 lb). The top displacement of those two specimens was less than 10% of the free height of the pole. Specimens 4, and 11 consisted of only 6 layers and weighed about 60 kg. Specimen 9, which also consisted of 6 layers but had a fiber orientation of 20°, failed at ultimate load 18.9 KN. This is less by 5% of that required for class 1, so this specimen was classified as class 2 pole. Five specimens (1, 3, 6, 7, and 8) exceeded the class 1 requirement and were classified in the heavier categories (H2 and H3). The maximum lateral displacement of pole was less than 12.7%.

Table (3): Performance of full-scale GFRP poles

Specimen Number	Weight (Kg)	Ultimate Capacity (KN)	Top Displacement (mm)	Equivalent Wooden Pole Class	Displacement As % of Free Height	Load/ Weight (KN/Kg)
1	99.40	34.2	486	H3	9.7	0.34
2	80.25	See Note				
3	68.15	30.1	608	H2	12	0.44
4	60.85	20.8	430	1	8.6	0.34
5	39.00	7.55	240	6	4.8	0.19
6	94.30	30.4	431	H2	8.6	0.32
7	81.00	36.4	634	H3	12.7	0.47
8	72.05	28.1	593	H2	11.9	0.39
9	59.40	18.9	416	2	8.3	0.32
10	38.20	6.9	252	6	5.0	0.18
11	62.50	20	403	1	8.1	0.32
12	38.00	8.8	278	5	5.6	0.23

Note: This specimen failed prematurely due to the lack of internal stiffener within the concrete base.

Since each specimen had a different weight and a different carrying capacity, the load capacity-to-weight ratio (KN/Kg) was used to compare the performance of different specimens. Specimen 7, which consisting of 8 layers (6 longitudinal layers and 2 circumferencial layers), had the highest performance ratio of approximately 0.47 KN/Kg. Specimens 3, and 8, which consisting of 8 layers (4 longitudinal layers and 4 circumferencial layers), had a load-to-weight ratio of 0.4 KN/Kg. Specimens 1, and 6, consisting of 8-longitudinal layer without any circumferencial ones, did not perform as well as the other 8-layer pole group and had a value of 0.32 KN/Kg.

A significant drop in performance ratio was observed when the number of layers was reduced to 6 or 4 layers. This was due to the high reduction in the wall thickness which in turn reduced the buckling load significantly, much more than the reduction the weight of the specimen. As shown Table 3, the weight ratio for specimen 4 was approximately, 0.34 KN/Kg. This is almost the same value as that specimen 1 that had 8 longitudinal layers without circumferencial layers. This indicate the importance of including circumferencial layers to achieve the same performance of pole having larger number of layers but with only longitudinal fibers.

Based on the dimensions of a class 1 wooden poles of total height 6.1 m (20 ft) the load capacity-to-weight ratio is 0.095 KN/Kg. The load-to-weight ratio for an equivalent class 1 GFRP pole (specimen 4 or 11) is 0.3 KN/Kg. This means that GFRP poles are more efficient than wooden poles and are approximately only one third of the weight of equivalent wooden poles.

All specimens with circumferencial layers (with the exception of specimen 2), failed by local buckling on the compression side of the specimens at a height which varied from 200 mm to 800 mm above the concrete base, as shown in Fig.2. Specimen 1, which had no circumferencial winding, also failed by local buckling on the compression side 200 m above the base and failure was combined with excessive splitting, and delamination of the fibers.

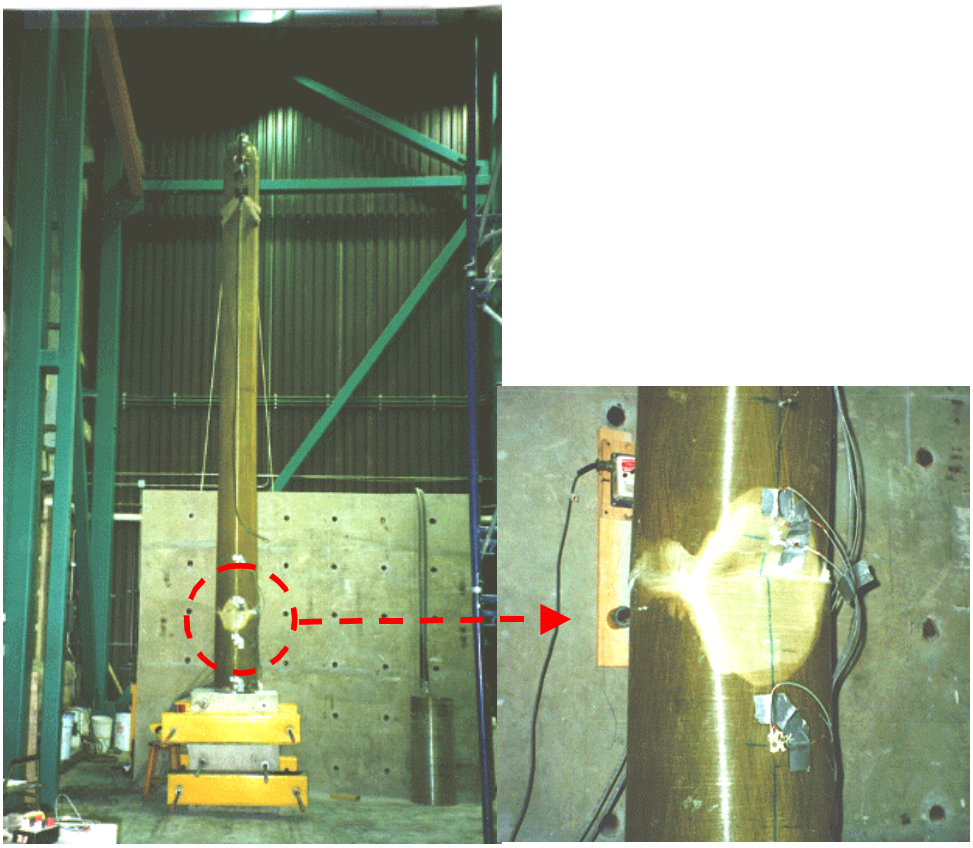

Fig.2: Local buckling failure mode

The failure mechanism of specimen 6 is shown Fig.3. A diagonal crack extending to a height between 200 mm to 1200 mm above the base developed on the compression side.

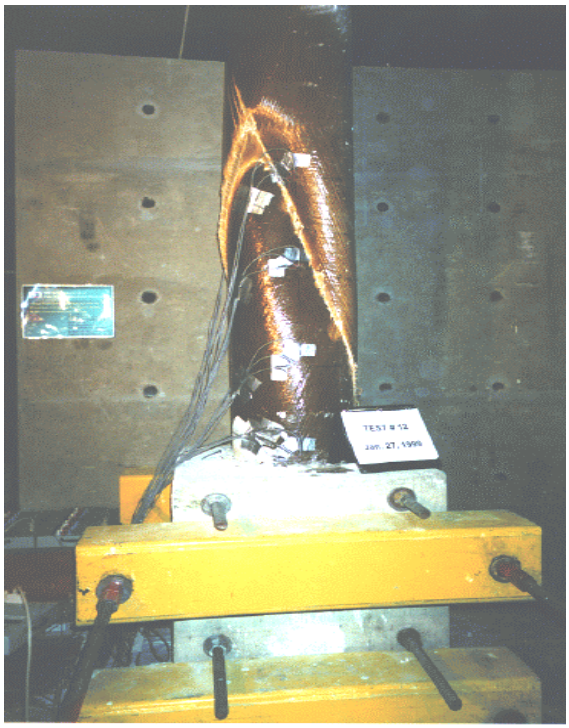

Fig. 3: Diagonal fracture failure mode

THEORETICAL ANALYSIS

The ANSYS program [6] was used to develop a nonlinear finite element model of GFRP poles. The geometric boundaries of the FRP poles were defined, as the first step in the modeling process. Eight-node quadrilateral layered shell element was used to model GFRP poles. Detailed formulation of this element is given by Ref. [7]. The portion of the specimen, which was embedded inside the concrete base, was also included in the model. In the current study, a geometric nonlinear analysis was used taking into account the cross section distortion as well as the large deflection at the top. The proposed model used to predict the ultimate failure load, whether it was due to instability (local buckling) or material failure. Fig. 4 shows a comparison between the experimental and the predicted ultimate loads for the tested specimens. The average ratio of the experimental-to-theoretical ultimate load was approximately 0.99 with a standard deviation of 12%. As evident from this figure, it is clear that there is a strong correlation between the results obtained from the proposed model and the experimental results.

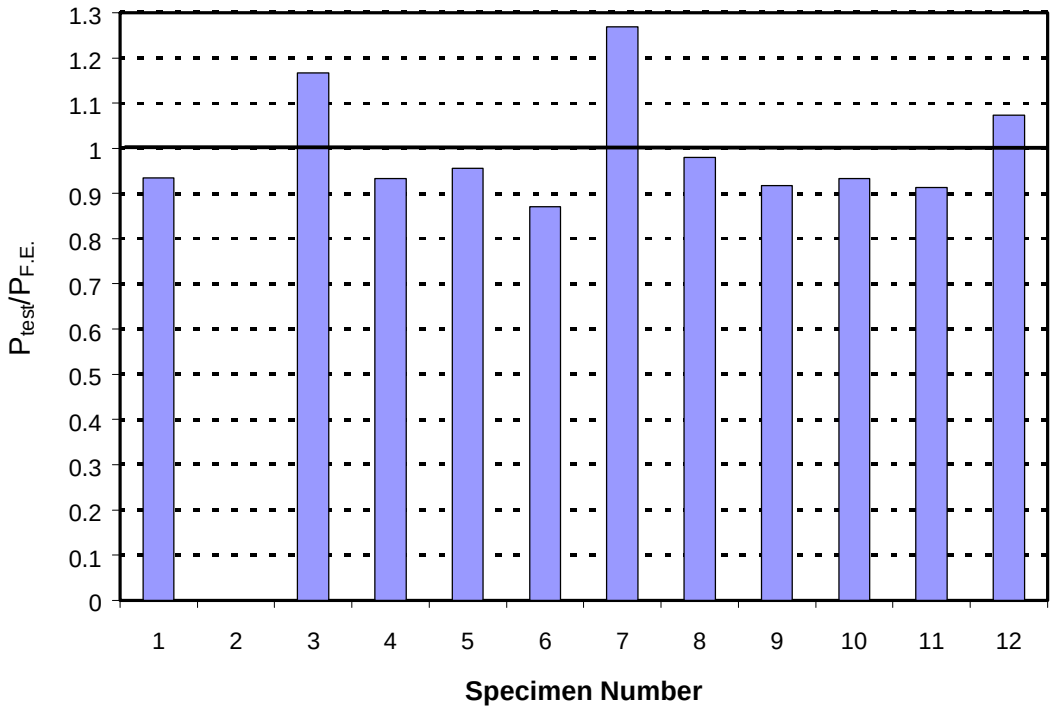

Fig. 4: Comparison between theoretical and experimental ultimate load

CONCLUSIONS

An experimental study was employed to investigate the ultimate capacity and performance of tapered filament wound GFRP poles subjected to cantilever bending. GFRP poles proved to carry the same ultimate load equivalent to wooden poles. However, a significant saving in the weight is achieved by utilizing GFRP. The load capacity-to-weight ratio of GFRP poles is almost three times higher than the equivalent wooden poles. Maximum load capacity-to-weight ratio was achieved by incorporating circumferencial winding along with longitudinal fibers. Amongst the 8-layer GFRP poles, the maximum load capacity-to-weight ratio was attained when only two circumferencial layers were combined with six longitudinal layers. Local buckling was the most dominant mode of failure in most of the specimens because of the high radius-to-thickness ratio of the specimens. On the other hand, only one specimen failed due to material failure on the compression side because of the absence of circumferencial layers in that specimen. The finite element method employed in this investigation provided an excellent prediction of the critical buckling and material failure loads as well as the corresponding modes of failure for thin-walled GFRP poles.

ACKNOWLEDGEMENT

The research project in this study was sponsored by ISIS-Canada, Faroex Ltd. of Manitoba, and The Province of Manitoba. The specimens were fabricated at the ISIS-Faroex filament winding Research Facility and the testing was conducted at the Structural Engineering and Construction R&D Facility at the University of Manitoba.

REFERENCES

1. Vanderbuilt, M. D. and Criswell, M. E., "Reliability Analysis of Pole-Type Transmission Structures" *Computer and Structures*, Vol. 6, No. 2, 1988, pp. 335-343.

2. McClure, G., Boire, L., and Carriere, J. C., "Applications of Advanced Composite Materials in Overhead Power Lines and Telecommunications Structures" *Advanced Composite in Bridges and Structures*, K.W. Neale and P. Labossiere, Editors, Canadian Society of Civil Engineering, 1992, pp.543-549.

3. Derrick, G. L., "Fiberglass Composite Distribution and Transmission Poles" *Manufactured Distribution and Transmission Pole Structures Workshop Proceeding*, Electric Power Research Institute, July 25-26, 1996, pp. 55-61.

4. Dow Plastics Company, "Technical Product Information", Midland, MI, 1997.

5. American National Standards Institute (ANSI), "American National Standard for Wood Poles 05.1" *Specifications and Dimensions*, 22 West 42nd Street, New York, 1992.

6. ANSYS, Inc., "ANSYS User's Manual for Revision 5.2 - Volumes I to IV" 1995, Houston, PA.

7. Yunus, S., Kohnke, P. C., and Saigal, S. "An Efficient Through-Thickness Integration Scheme in Unlimited Layered Doubly Curved Isoparametric Composite Shell Element" *International Journal for Numerical Methods In Engineering*, Vol. 28, 1989, pp. 2777-2793.